DOI: 10.61782/fa.2023.0663

forum acusticum 2023

IMPERFECT INTERFACES CHARACTERIZATION IN A MULTILAYERED STRUCTURE BY MEANS OF AN EQUIVALENT DYNAMIC MODEL

Nicolas AUQUIER[1,2,3,*] **Kerem EGE**[1,2] **Emmanuel GOURDON**[1,3]

[1] LabEx CeLyA - Centre Lyonnais d'Acoustique, 36, avenue Guy de Collongue, 69134, Ecully, France
[2] Univ Lyon, INSA Lyon, LVA, EA677, 69621 Villeurbanne, France
[3] Univ Lyon, ENTPE, Ecole Centrale de Lyon, CNRS, LTDS, UMR5513 69518, Vaulx-en-Velin, France

ABSTRACT

This work aims to characterize the dynamical behavior of a multilayered beam with imperfect interfaces thanks to an equivalent model. The imperfect interfaces studied are a result of the coupling conditions of the layers, modelled by a spring and a discontinuity of the displacement. Such modelling is able to consider the transition between a perfectly bonded and a fully debonded multilayered structure. The resulting model is used to characterize experimental samples by an inverse method. The samples used are manufactured to have a decreasing quality of the coupling within the multilayered beam, to compare the behavior of the coupling conditions. The samples are made of glass and epoxy in order to have an overview of the interface quality. The Corrected Force Analysis Technique (CFAT) is used to characterize the samples and check the effect of imperfect interfaces. The characterization is done by estimating the apparent bending stiffness of the sample and the corresponding losses thanks to the measured velocity. The measurements are performed by means of a Laser Doppler Vibrometer (LDV).

Keywords: *imperfect interface, characterization, multilayered, equivalent model*

Corresponding author: *nicolas.auquier@insa-lyon.fr.*

1. INTRODUCTION

Equivalent models are commonly used to study the dynamics of multilayered structures [1–4]. The goal is to describe with few parameters the whole behavior of such structures, which can be a good alternative to Finite Element Method (FEM). In this work, an equivalent model with imperfect interfaces recently published [5] is used to characterize imperfect sandwich beams. The model used is an Equivalent Singler Layer (ESL) model, based on Guyader–Marchetti model [6, 7]. Such models describe the whole multilayered plate with respect to a reference layer, hereby reducing drastically the amount of variables of the system to solve. This is done usually thanks to continuity conditions at the interfaces between the layers. However, to implement imperfect interfaces, the displacement field is assumed to be discontinuous as in [8–10]. A constitutive equation is used to write the stresses within the multilayered structure with respect to the sliding displacement thanks to a spring approach. The stiffness of the spring symbolizes the quality of the coupling between the layers at the interface and impact the overall behavior of the system as shown experimentally in [11–14].

This work aims to highlight the imperfect interfaces impact on the dynamics of a multilayered structure from the measurement itself. To do so, an experimental dynamic characterization of imperfect interfaces samples is performed, thanks to vibration measurement and model fitting. Details about the post processing of the data, in particular the filtering, are given here since they greatly

enhance the quality of the results and so increase the bandwidth of the results. The samples boundary conditions are free-free, which is accomplished by using ropes to suspend it. Vibration of the system is generated by means of at least two piezoelectric buzzers. The data obtained from the measurement are processed according to the Corrected Force Analysis Technique (CFAT) [15, 16].

The originality of this work is to show the impact of imperfect coupling between the layers of a sandwich structure experimentally over a broadband frequency, which enables modal analysis and wave analysis. This paper is organized as follow: The Section 2 shows the main characteristics of the equivalent model used here. The experimental setup is briefly shown in Section 3. Section 4 gives details about the methodology used in this work, so mainly details about the data filtering method. The results of the experimental study are shown in a separated part, namely Section 5.

2. MODEL

This section is a brief summary of [5], the reader is referred to this paper for more details. The main equation of the model, for a beam, is the Equation (1). It yields the displacement field to be modelled thanks to 4 terms: the extension over x $\psi_x(x,t)$; the bending over x $\frac{\partial W}{\partial x}$; the shearing ϕ_x; and the displacement jump $\hat{u}_x$, which is assumed to be constant over the surface (x, y) and with respect to the time t.

$$\begin{cases} u_x^n = \psi_x^1(x,t) + F_\omega \frac{\partial W}{\partial x} + F_{xx}^n \phi_x^1 + \sum_{i=1}^n \hat{u}_x^i, \\ u_z^n = W(x,t). \end{cases} \tag{1}$$

With F_{xx}^n function of the Young's modulus of the layers and their thicknesses, details in [5–7, 17]. Then, the displacement jumps are computed thanks to the constitutive law, Equation (2).

$$\hat{u_x}^n_{z=z^n} = B_{xz}^n \hat{\sigma}_{xz}^n, \tag{2}$$

With, B_{xz}^n the interface compliance in the x direction generally called the interface parameter.

This yields the displacement field to be written exclusively by the kinematic variables of Eq. (3). If ${B_{xz}}^n = 0$ m.Pa^{-1} the interface is perfect since the displacement obtained is the same as in the former models. If $B \to \infty$, or the interface stiffness $K_{xz} = 1/B_{xz} \to 0$ Pa.m^{-1}, the interface is fully debonded.

$$\begin{cases} u_x^n = \psi_x^1(x,t) + F_\omega \frac{\partial W}{\partial x} + F_{xx_g}^n \phi_x^1 - \sum_{i=1}^n B_{xz}^i t_x^i, \\ u_z^n = W(x,y,t). \end{cases} \tag{3}$$

3. EXPERIMENTAL SETUP

The experimental setup is fully presented in Figure 1. The samples manufactured for this study are sandwich-structured beams. The skins have the same thickness and are made of glass, which is useful to directly see the quality of the interfaces. The core is ten times thinner than the skins and is made of a hard epoxy adhesive, which is a viscoelastic material with a high Young's modulus ($E_{core} \approx 2$ GPa) relatively to similar materials. The velocity measurements are performed by means of a Laser Doppler Vibrometer (LDV) from Polytec, the PSV-400. A piezoelectric buzzer is glued to the sample in order to make it vibrates. The resulting velocity is measured throughout a mesh by means of the PSV-400 scanning vibrometer from Polytec. The input signal is a white noise with $f = [1e3, 1e5]$ Hz.

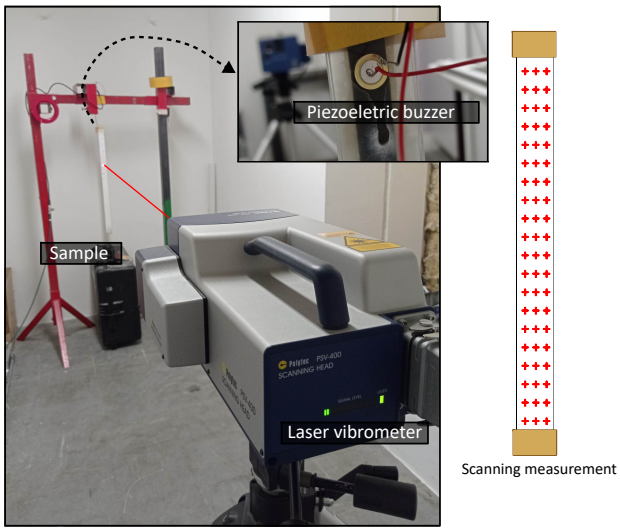

Figure 1. Experimental setup with a picture of the setup itself with: the scanning laser vibrometer PSV-400 Polytec; the glass-epoxy-glass sample in free vibration; the piezoeletric buzzer glued to the sample. A scheme of the sample with the scanning mesh is represented on the right of the picture.

	Skins	Core
Thickness [mm]	3	0.3
Young's modulus [GPa]	71	1.5
Damping [-]	0.1e-2	5e-2
Poisson ratio [-]	0,33	0,22
Density [kg.m-3]	2700	1300

Table 1. Mechanical properties of the materials composing the sandwich structured beam.

The sample properties used for this work are gathered in Table 1 and are shown Figure 2.

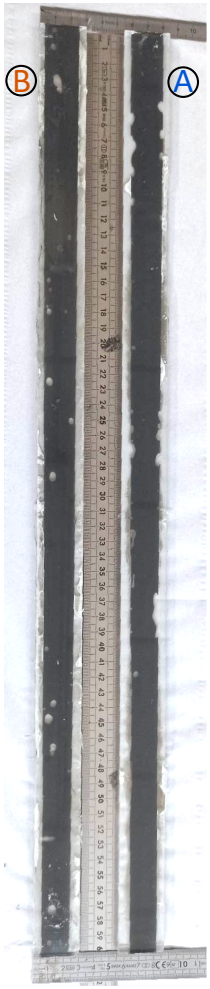

Figure 2. Samples A and B. They both have the same geometry (600x30x0.3mm^3) and mechanical properties (Glass-Epoxy-Glass Table 1), except the amount of epoxy used to couple both skins. The epoxy mass of Sample A is $m_{2_A} = 9.4$g and $m_{2_A} = 9.8$g .

4. METHODOLOGY

4.1 Corrected Force Analysis Technique (CFAT)

The data processing used to compute the flexural rigidity of the samples is the Corrected Force Analysis Technique, few more implementation of the method are given in [15, 16, 18]. This method uses the vertical displacement equation of motion of a beam (or a plate if needed). In order to characterize the apparent mechanical parameters of the sample in the (x, y), it is assumed that the external pressure is null. Finally, Equation (4) is used to apply the method to a beam-like structure.

$$\frac{EI}{\rho S} = \omega^2 \Delta^4 \left[acos(1 - \frac{\Delta^2}{2} \sqrt{\frac{\delta_\Delta^{4x}}{w(x)}} \right]^{-4}, \qquad (4)$$

With, E Young's modulus, I, ω the frequency in rad.m^{-1}, Δ the mesh pitch, δ_Δ^{4x} is the 4^{th} derivative of the vertical displacement, it is estimated thanks to a finite difference method.

4.2 Experimental border-padding and filtering

The results on unfiltered data are given in Figures 5-6 in blue. One can notices that the results are reliable for the highest frequencies. This these discrepancies come from other type of strain taking into account from the original data. The wavenumber map given in Figure 3 shows that not only the flexural motion is measured, but other strains with lower wavenumbers.

Thus, filtering the data is necessary to enhance the results, which increase the bandwidth of the results. The issue when dealing with wavenumber filtering is the window application in low frequency. Since the resolution is rarely high enough for low frequency windowing, it yields bad results if no padding is added. To correct this, experimental border-padding has been realized with respect to the workflow given in Figure 4. The filtering itself, is done by a double convolution in the two directions. Since the convolution makes a phase shift, if the filtering is done twice in opposite directions, the two phase shifts are cancelling each other, leaving the imaginary part unchanged but filtered. Zero-padding is firstly done, then, cycles of

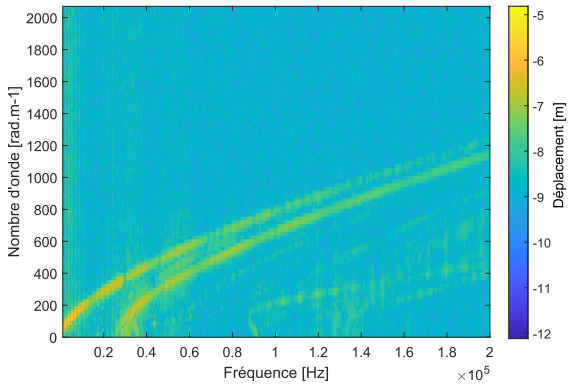

Figure 3. Wavenumber map obtained after measurement. The ordinate is the wavenumber of the plate, the abscissa the frequency and the colormap is the displacement amplitude.

filtering are processed by reusing the measure displacement for each loop. This yields the data to be gradually a border-padding obtained from experimental data only.

5. RESULTS

5.1 Filtering results

Results for the real part, the flexural rigidity modulus in Pa, and for the imaginary part, the flexural damping without units, are given respectively in the Figure 5 and the Figure 6. The flexural rigidity modulus is an equivalent Young's modulus for bending. It is computed from the structural beam parameter $s = E_{eq}I/(\rho S)$, $E_{eq} = 12s\rho/h^2$.

The results show the apparent flexural rigidity modulus and its damping with respect to the frequency. It is classical results for a multilayered structure. In low frequency, the bending makes only the hard skins involved in the dynamical behavior, but weighted by the full thickness. In the high frequency limits, the multilayered is fully debonded and the rigidity is greatly reduced since it equals the sum of the flexural rigidity of each layer weighted by their own thickness. The real part filtering shows really good improvement. The imaginary part filtering removes an unexpected collapse of the damping after 10^4 Hz, but adds a singularity at 12 kHz. In the highest frequencies the damping is not significantly improved since it is already very low, knowing that the imaginary part is more

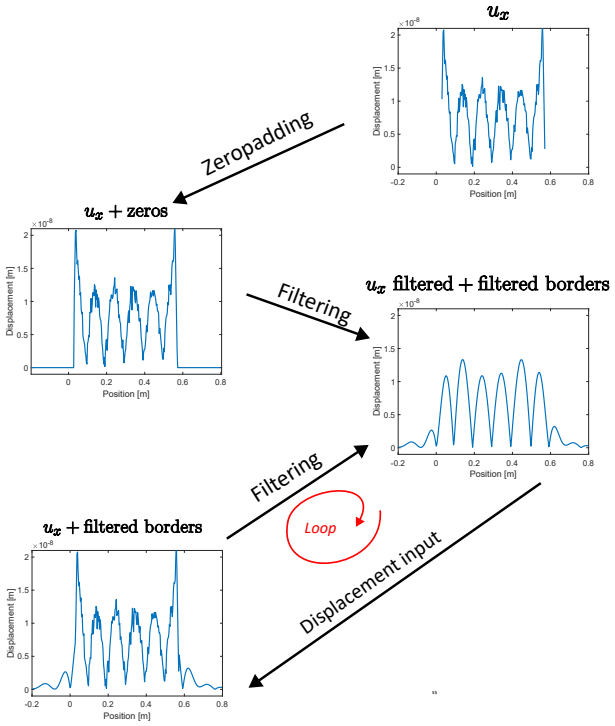

Figure 4. Workflow of the filtering method including border-padding.

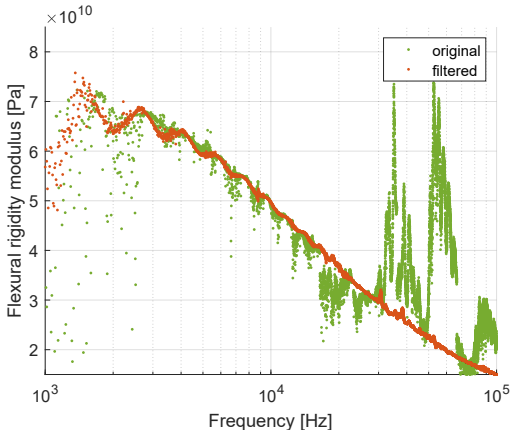

Figure 5. Impact of the filtering method presented in Section 4 on the Flexural rigidity modulus with respect to the frequency. The properties of the samples are gathered in Table 1.

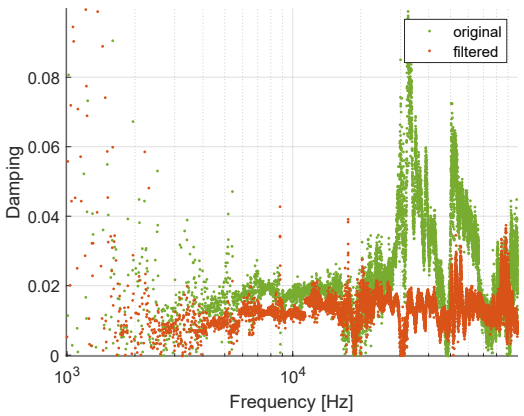

Figure 6. Impact of the filtering method presented in Section 4 on the damping with respect to the frequency. The properties of the samples are gathered in Table 1.

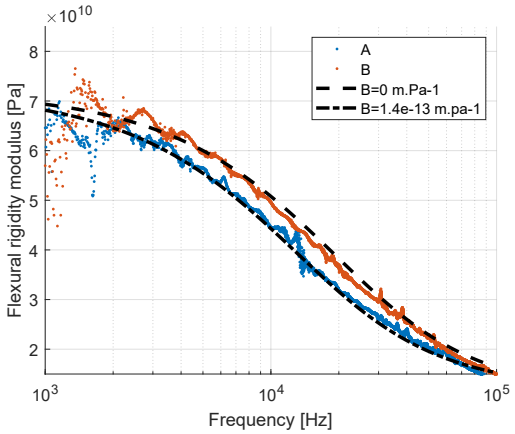

Figure 7. Impact of the imperfect interfaces on the flexural rigidity modulus with respect to the frequency. The samples have the same properties (Table 1) but their interface parameter B_{xz}.

sensitive to noise than the real part.

5.2 Imperfect interfaces impact on dynamical parameters

Now that the results are on a frequency broadband, it is possible to compare two multilayered structures with the same properties but the quality of their interfaces. Their properties are the same than for the filtering application, namely Table 1.

The samples used for the results shown in this section are shown in Figure 2. It shows two samples with the same properties but the amount of epoxy used for the core. The sample A has less epoxy than sample B, which makes sample A expected to be the sample with the worst coupling conditions. Since the thickness of the core is of 0.3mm, the lack of epoxy generates some defects inside the core (air inclusions) and some irregularities on the width, reducing hereby the coupling quality of the interface.

Figures 7-8 show the comparison between these two cases with sample A the least perfect sample, versus sample B the most perfect sample. Since the core properties were not perfectly known, sample B is assumed to have perfectly bonded interfaces, so as to set the values of the core. If one wants to precisely characterize the interface parameter, one has to know with similar precision than the skins, the properties of the core.

The results for the real part is well fitted by the model

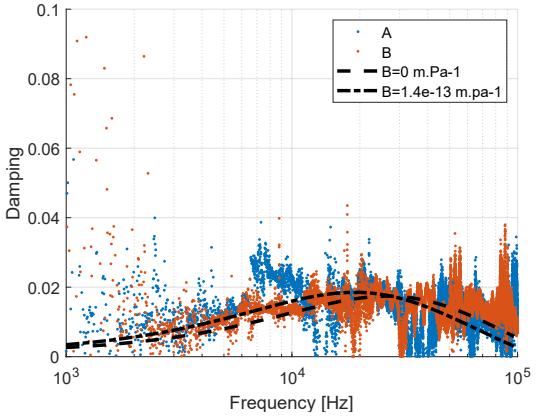

Figure 8. Impact of the imperfect interfaces on the damping with respect to the frequency. The samples have the same properties (Table 1) but their interface parameter B_{xz}.

with two different interface parameters. For the damping, the prediction of the experimental result trends by the model is acceptable, but the different singularities make impossible to have a prediction as good as for the real part all along the spectrum.

6. CONCLUSION

In this work, broadband characterization of imperfect interfaces has been shown. This implies the use of an experimental border-padding, and the use of an equivalent dynamic model to fit a vibration measurement performed with a laser vibrometer from $f = 1$k Hz to $f = 500$ kHz. Good agreement between the results and the model has been shown all along the frequency spectrum. However, the results for the imaginary part can still be improved. If not by data processing, it could be more accurate by using samples with a higher damping. This can be done by using another core material, or by increasing significantly its thickness.

7. ACKNOWLEDGMENTS

This work was supported by the LabEx CeLyA ("Centre Lyonnais d'Acoustique," Grant No. ANR10-LABX-0060) operated by the French National Research Agency. The authors would like to thank Julien Chatard, Laboratory Technician at LVA, for his precious help to manufacture the samples and Teddy Sacco, Mechanical Engineer, for his help during his internship by manufacturing more samples and measuring them. We also thank Quentin Leclère, Assistant Professor at LVA, for his precious knowledge about the data processing. We express our gratitude to Fabien Marchetti and Fabien Chevillote, Research Engineers at Matelys (Research Lab), for fruitful discussions.

8. REFERENCES

[1] E. Carrera, "An assessment of mixed and classical theories on global and local response of multilayered orthotropic plates," *Composite Structures*, vol. 50, pp. 183–198, Oct. 2000.

[2] S. Ghinet and N. Atalla, "Modeling thick composite laminate and sandwich structures with linear viscoelastic damping," *Computers & Structures*, vol. 89, pp. 1547–1561, Aug. 2011.

[3] K. Viverge, *Modèle de plaques stratifiées à fort contraste: application au verre feuilleté*. PhD thesis.

[4] U. Arasan, F. Marchetti, F. Chevillotte, G. Tanner, D. Chronopoulos, and E. Gourdon, "On the accuracy limits of plate theories for vibro-acoustic predictions," *Journal of Sound and Vibration*, vol. 493, p. 115848, Feb. 2021.

[5] N. Auquier, K. Ege, and E. Gourdon, "Equivalent dynamic model of multilayered structures with imperfect interfaces: Application to a sandwich structured plate with sliding interfaces," *Journal of Sound and Vibration*, vol. 535, p. 117052, Sept. 2022.

[6] J. Guyader and C. Lesueur, "Acoustic transmission through orthotropic multilayered plates, part II: Transmission loss," *Journal of Sound and Vibration*, vol. 58, pp. 69–86, May 1978.

[7] F. Marchetti, *Modélisation et caractérisation large bande de plaques multicouches anisotropes*. Vibrations, Institut National des Sciences Appliquées de Lyon (INSA Lyon), France, 2019.

[8] D. Liu, L. Xu, and X. Lu, "Stress analysis of imperfect composite laminates with an interlaminar bonding theory," *International Journal for Numerical Methods in Engineering*, vol. 37, pp. 2819–2839, Aug. 1994.

[9] Z.-q. Cheng, A. K. Jemah, and F. W. Williams, "Theory for Multilayered Anisotropic Plates With Weakened Interfaces," *Journal of Applied Mechanics*, vol. 63, pp. 1019–1026, Dec. 1996.

[10] R. Massabò and F. Campi, "An efficient approach for multilayered beams and wide plates with imperfect interfaces and delaminations," *Composite Structures*, vol. 116, pp. 311–324, Sept. 2014.

[11] M. Schoenberg, "Elastic wave behavior across linear slip interfaces," *The Journal of the Acoustical Society of America*, vol. 68, pp. 1516–1521, Nov. 1980.

[12] A. I. Lavrentyev and S. I. Rokhlin, "Ultrasonic spectroscopy of imperfect contact interfaces between a layer and two solids," *The Journal of the Acoustical Society of America*, vol. 103, pp. 657–664, Feb. 1998.

[13] A. I. Lavrentyev and J. T. Beals, "Ultrasonic measurement of the diffusion bond strength," *Ultrasonics*, vol. 38, pp. 513–516, Mar. 2000.

[14] F. J. Margetan, R. B. Thompson, J. H. Rose, and T. A. Gray, "The interaction of ultrasound with imperfect interfaces: Experimental studies of model structures," *Journal of Nondestructive Evaluation*, vol. 11, pp. 109–126, Dec. 1992.

[15] Q. Leclère and C. Pézerat, "Vibration source identification using corrected finite difference schemes," *Journal of Sound and Vibration*, vol. 331, pp. 1366–1377, Mar. 2012.

[16] Q. Leclère, F. Ablitzer, and C. Pézerat, "Practical implementation of the corrected force analysis technique to identify the structural parameter and load distributions," *Journal of Sound and Vibration*, vol. 351, pp. 106–118, Sept. 2015.

[17] A. Loredo and A. Castel, "A multilayer anisotropic plate model with warping functions for the study of vibrations reformulated from Woodcock's work," *Journal of Sound and Vibration*, vol. 332, pp. 102–125, Jan. 2013.

[18] K. Ege, N. Roozen, Q. Leclère, and R. G. Rinaldi, "Assessment of the apparent bending stiffness and damping of multilayer plates; modelling and experiment," *Journal of Sound and Vibration*, vol. 426, pp. 129–149, July 2018.